Supplementary Information

Maxime Boudjelel,[a] Sonia Mallet–Ladeira,[b] Ghenwa Bouhadir[a] and Didier Bourissou[a]*

[a] CNRS / Université Paul Sabatier, Laboratoire Hétérochimie Fondamentale et Appliquée (LHFA, UMR 5069). 118 Route de Narbonne, 31062 Toulouse Cedex 09 (France)

[b] Institut de Chimie de Toulouse (FR 2599). 118 Route de Narbonne, 31062 Toulouse Cedex 09 (France)

Corresponding Author: dbouriss@chimie.ups-tlse.fr

Contents

General comments

All reactions and manipulations were carried out under an atmosphere of dry argon using standard Schlenk techniques or a glovebox. All solvents were sparged with argon and dried using an MBRAUN Solvent Purification System (SPS). All solvents were degassed using freeze pump technique. ^{1}H, ^{13}C, ^{31}P, ^{11}B and ^{19}F NMR spectra were recorded on a Bruker Avance III HD 500 (equipped with a prodigy probe), Avance III HD 400, Avance II 300 and Avance I 300 spectrometers. Chemical shifts are expressed with a positive sign, in parts per million, calibrated to residual ^{1}H and ^{13}C solvent signals. External $BF_3.OEt_2$, 85% H_3PO_4 and $CFCl_3$ were used as reference for ^{11}B, ^{31}P and ^{19}F NMR respectively. Mass spectra were recorded on a Waters LCT mass spectrometer. Elemental analyses were recorded on a ThermoFisher Flash 1112 hosted at Centre Régional de Mesures Physiques de l'Ouest. IR spectroscopy was recorded on a IR-TF Thermo Scientific™ Nicolet™ iS™ 50 using a CaF_2 cuvette.

Ligand **1** was prepared following the reported procedure.[1] All others reagents were purchased from Sigma-Aldrich or Fluorochem and used as received. TlCp was sublimed just before used.

The Fxyl and Xyl abbreviations are used for the 3,5-bis(trifluoromethyl)phenyl and 2,6-dimethylphenyl substituent, respectively.

[1] Boudjelel, M. ; Carrizo, E. D. S.; Mallet−Ladeira, S.; Massou, S.; Miqueu, M.; Bouhadir, G.; Bourissou, D. *ACS Catal.* **2018**, *8*, 4459−4464.

Synthesis of the (Cp)Rh(P,B) complex **2**

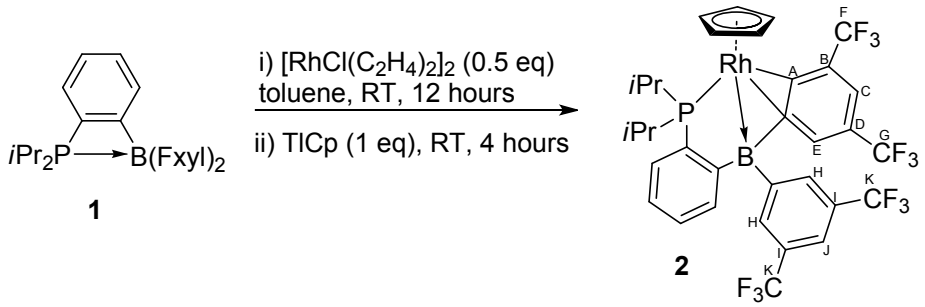

1 (100 mg, 0.159 mmol) and $[RhCl(C_2H_4)_2]_2$ (31 mg, 0.080 mmol) were charged in a vial in the glovebox. The powders were dissolved in 5 mL of toluene and the reaction was left to stir in the glovebox for 12 hours. TlCp (43 mg, 0.160 mmol) was then added as a solid in the reaction medium. After 4 hours of stirring, the deep purple solution was removed from the white precipitate of Thallium Chloride using a PTFE filter (UptiDisc ™ 0.20 μm), and the purple filtrate was left in a closed vial at room temperature. After 12 hours, the product started to crystallize. The vial was then cooled at -22°C. After 12 hours, crystals were collected and washed with 1 mL of toluene. Crystals were dried under high vacuum to retrieve 86 mg of a deep purple powder (68% yield). X-Ray quality crystals were obtained by slow evaporation of a concentrated pentane solution at room temperature.

HRMS (ES-MS$^+$): exact mass (monoisotopic) calcd. for $[M]^+$ $(C_{33}H_{29}PF_{12}BRh)^+$: 798.0969; found: 798.0980.

Elemental Analysis was obtained directly from the NMR sample used for the characterization of the compound, which explains the presence of 0.25 equivalent of CD_2Cl_2.
Anal. Calcd. for $C_{33}H_{29}BF_{12}PRh.0.25CD_2Cl_2$: C, 48.70; H, 3.56. Found: C, 48.78; H, 3.41.

m.p.: 120 °C.

^{1}H NMR (300 MHz, CD_2Cl_2, 293K, δ): 0.58 (dd, 3H, $^3J_{HP}$ = 17.0 Hz, $^3J_{HH}$ = 7.0 Hz, CH_{3iPr}), 1.08 (dd, 3H, $^3J_{HP}$ = 13.0 Hz, $^3J_{HH}$ = 7.0 Hz, CH_{3iPr}), 1.31 (dd, 3H, $^3J_{HP}$ = 17.0 Hz, $^3J_{HH}$ = 7.0 Hz, CH_{3iPr}), 1.43 (dd, 3H, $^3J_{HP}$ = 15.0 Hz, $^3J_{HH}$ = 7.0 Hz, CH_{3iPr}), 2.16 (m, 1H, CH_{iPr}), 2.85 (m, 1H, CH_{iPr}), 3.53 (br s, 1H, H_A), 4.77 (s, 5H, Cp), 7.21-7.41 (m, 5H, H_{arom}+H_C), 7.77 (s br, 1H, H_J), 8.43 (s br, 1H, H_E), 8.53 (s br, 2H, H_H).

^{13}C{^{1}H} NMR (100 MHz, CD_2Cl_2, 293K, δ): 17.32 (d, $^2J_{CP}$ = 6.0 Hz, CH_{3iPr}), 17.94 (d, $^2J_{CP}$ = 3.0 Hz, CH_{3iPr}), 18.22 (m, CH_{3iPr}), 20.61 (d, $^2J_{CP}$ = 3.0 Hz, CH_{3iPr}), 25.27 (d, $^1J_{CP}$ = 26.0 Hz, CH_{iPr}), 31.46 (d, $^1J_{CP}$ = 28.0 Hz, CH_{iPr}), 61.43 (br d, $^1J_{CRh}$ = 9.0 Hz, C_A), 90.94 (dd, $^1J_{CRh}$ = 4.0 Hz, $^2J_{CP}$ = 1.6 Hz, Cp), 118.18 (m, C_C), 119.91 (hept, $^3J_{CF}$ = 3.8 Hz, C_J), 124.34 (q, $^1J_{CF}$ = 274.0 Hz, C_F), 124.54 (q, $^1J_{CF}$ = 272.0 Hz, C_G), 124.69 (q, $^1J_{CF}$ = 271.0 Hz, $2C_K$), 124.96 (q, $^2J_{CF}$ = 32.0 Hz, C_B), 126.45 (d, J_{CP} = 6.6 Hz, CH_{arom}), 129.59 (m, CH_{arom}), 130.07 (q, $^2J_{CF}$ = 32.0 Hz, $2C_I$), 130.26 (d, J_{CP} = 2.5 Hz, CH_{arom}), 132.11 (dd, $^1J_{CP}$ = 47.0 Hz, $^2J_{CRh}$ = 1.4 Hz, $C_{ipso}P$), 132.57 (d, J_{CP} = 21.5 Hz, CH_{arom}), 135.67 (m, C_H), 137.18 (q, $^2J_{CF}$ = 32.0 Hz, C_D), 143.16 (m, C_E). N.B.: $C_{ipso}B$ quaternary carbon atoms were not observed.

^{11}B NMR signal was not observed.

^{31}P{^{1}H} NMR (121 MHz, CD_2Cl_2, 293K, δ): 79.62 (d, $^1J_{PRh}$ = 173 Hz).

^{19}F NMR (376 MHz, CD_2Cl_2, 293K, δ): -64.20 (s, C_FF_3), -63.99 (s, C_GF_3), -63.06 (s, $2C_KF_3$).

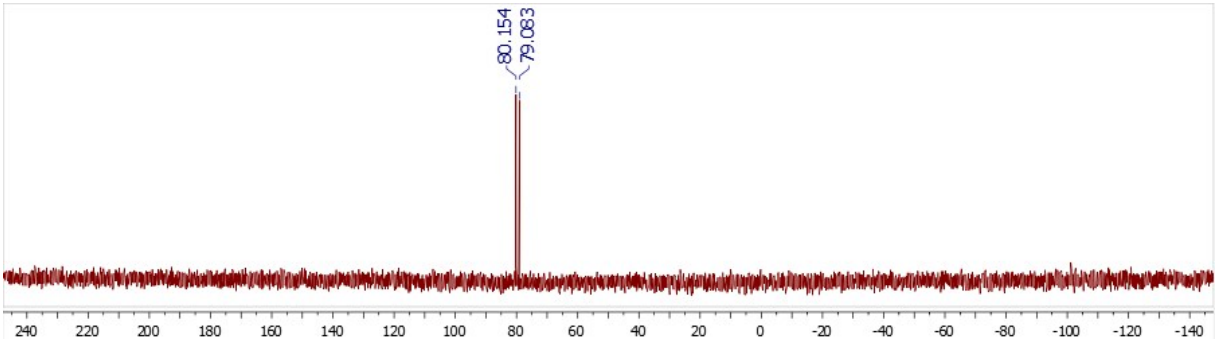

Figure S1. $^{31}P\{^{1}H\}$ NMR spectrum of **2** (171 MHz, 293K) in CD_2Cl_2

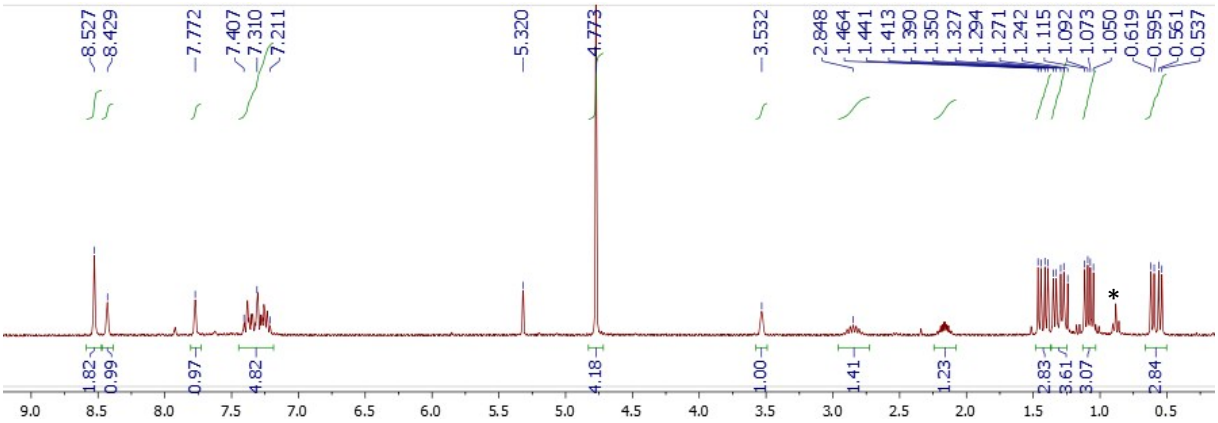

* Pentane

Figure S2. ^{1}H NMR spectrum of **2** (300 MHz, 293K) in CD_2Cl_2

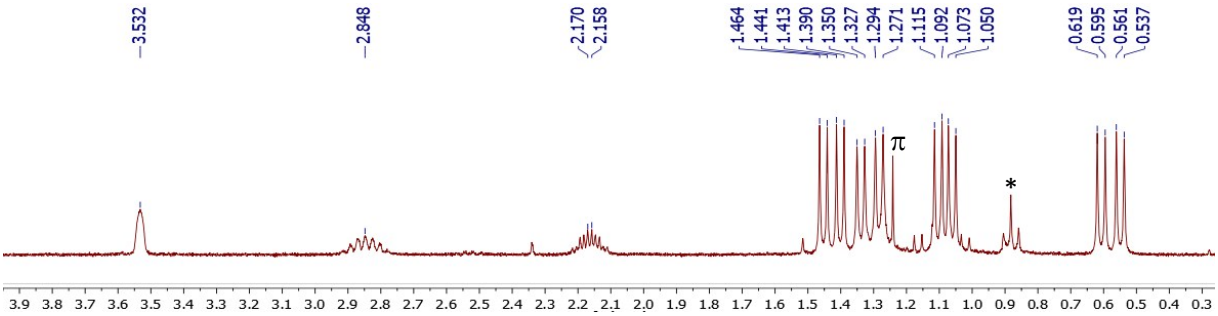

* Pentane, π unidentified impurity.

Figure S3. ^{1}H NMR spectrum of **2** (300 MHz, 293K) in CD_2Cl_2, aliphatic region

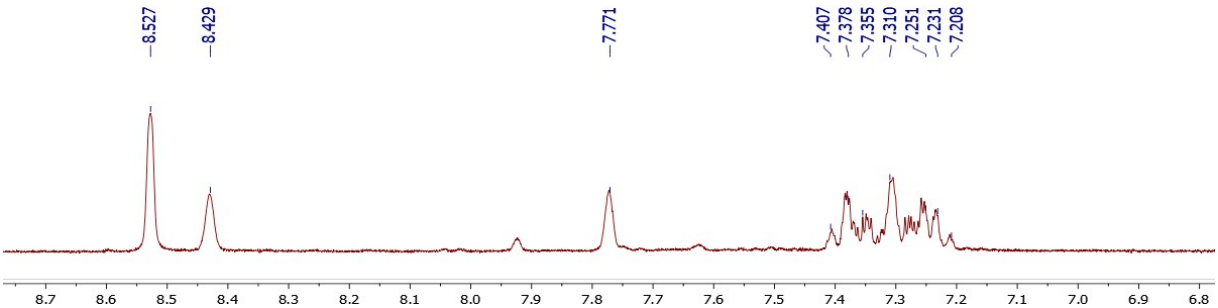

Figure S4. ^{1}H NMR spectrum of **2** (300 MHz, 293K) in CD_2Cl_2, aromatic region

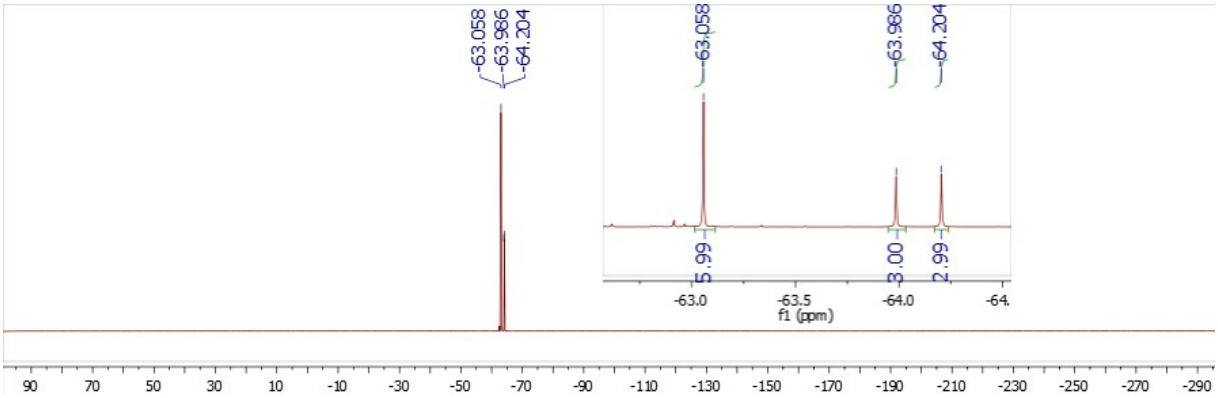

Figure S5. ^{19}F NMR spectrum of **2** (376 MHz, 293K) in CD_2Cl_2

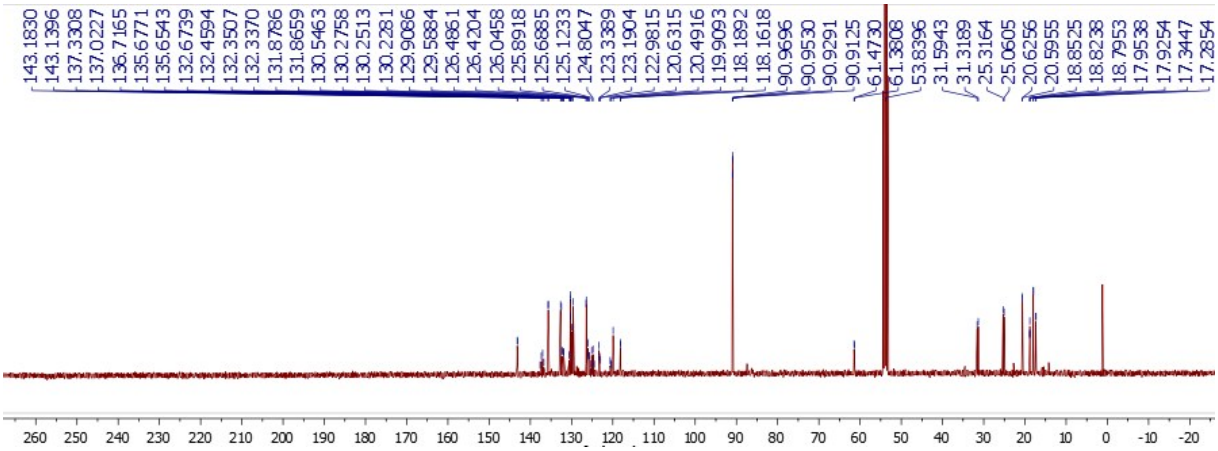

Figure S6. $^{13}C\{^1H\}$ spectrum of **2** (100 MHz, 293K) in CD_2Cl_2

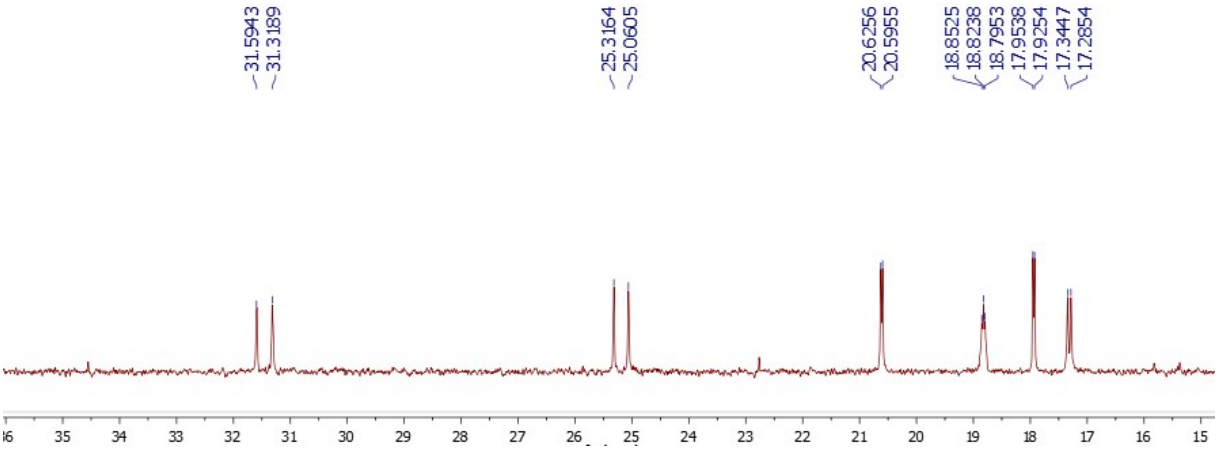

Figure S7. $^{13}C\{^1H\}$ spectrum of **2** (100 MHz, 293K) in CD_2Cl_2; aliphatic region

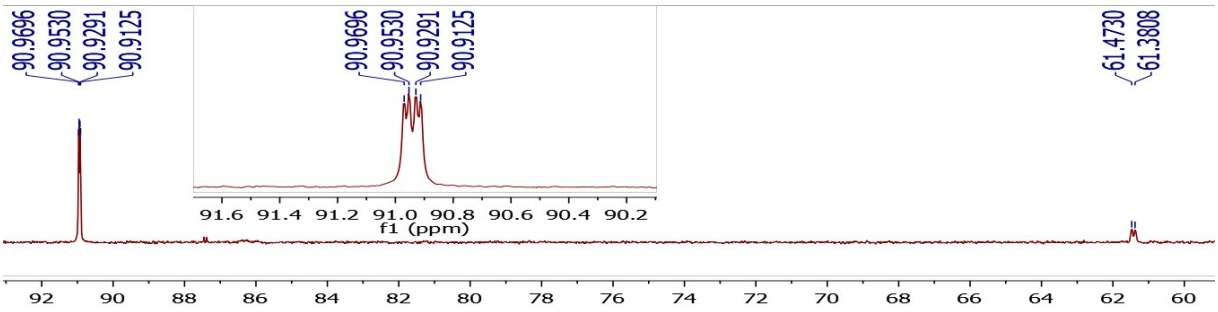

Figure S8. $^{13}C\{^{1}H\}$ spectrum of **2** (100 MHz, 293K) in CD_2Cl_2; Cp region

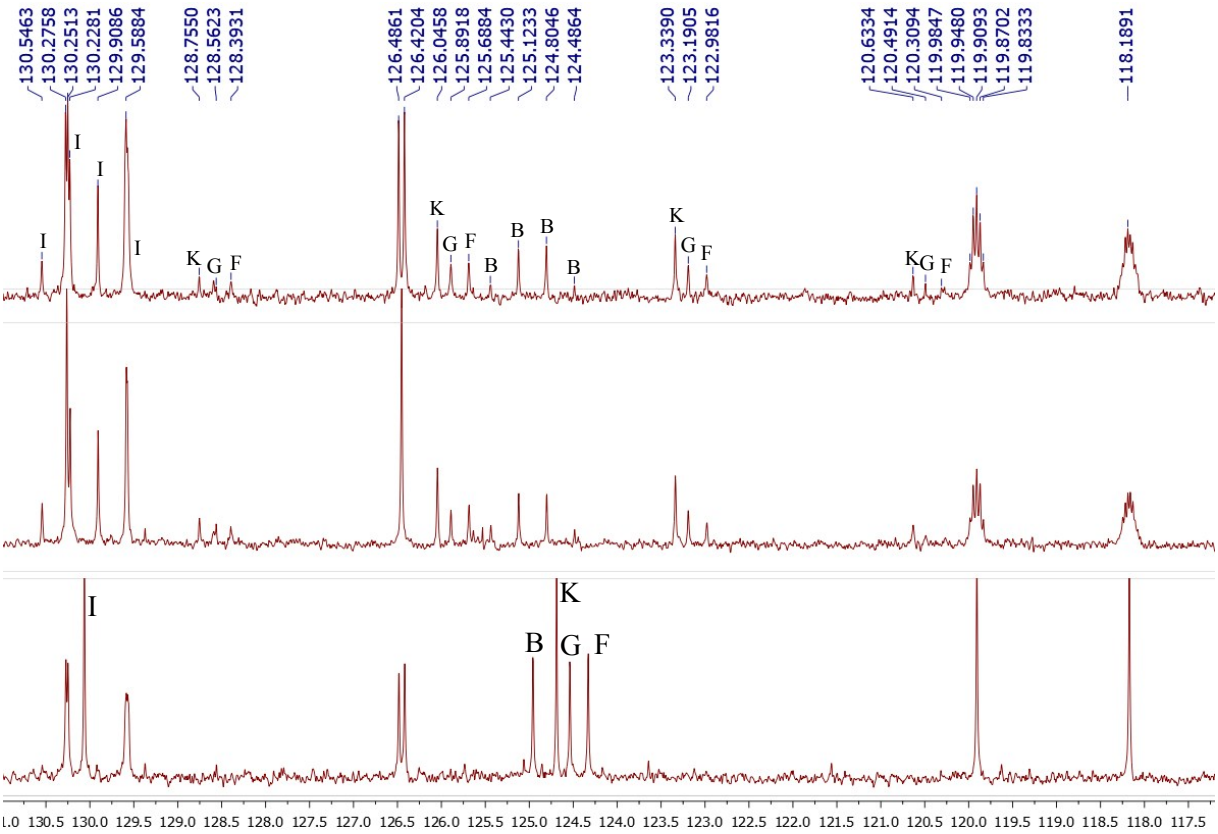

Figure S9. $^{13}C\{^{1}H\}$ spectrum of **2** (100 MHz, 293K) in CD_2Cl_2; aromatic region, zoom 1 Top $^{13}C\{^{1}H\}$, middle $^{13}C\{^{1}H,^{31}P\}$, bottom $^{13}C\{^{1}H,^{19}F\}$.

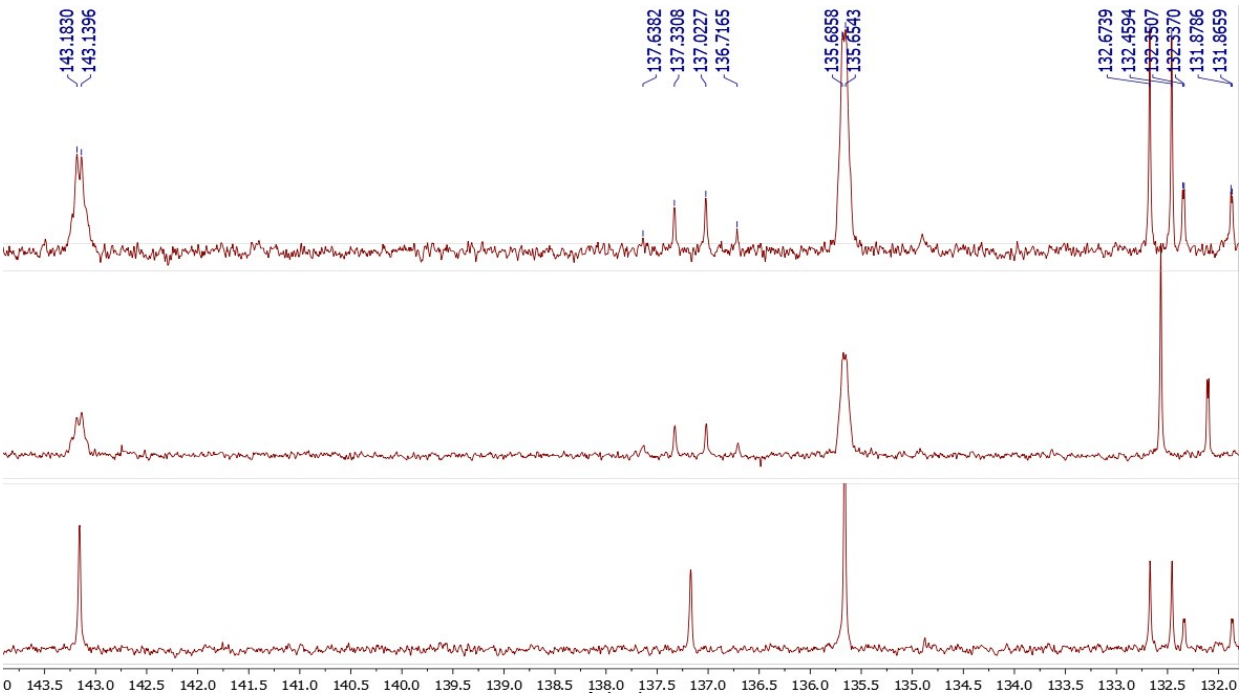

Figure S10. $^{13}C\{^{1}H\}$ spectrum of **2** (100 MHz, 293K) in CD_2Cl_2; aromatic region, zoom 2 Top $^{13}C\{^{1}H\}$, middle $^{13}C\{^{1}H,^{31}P\}$, bottom $^{13}C\{^{1}H,^{19}F\}$.

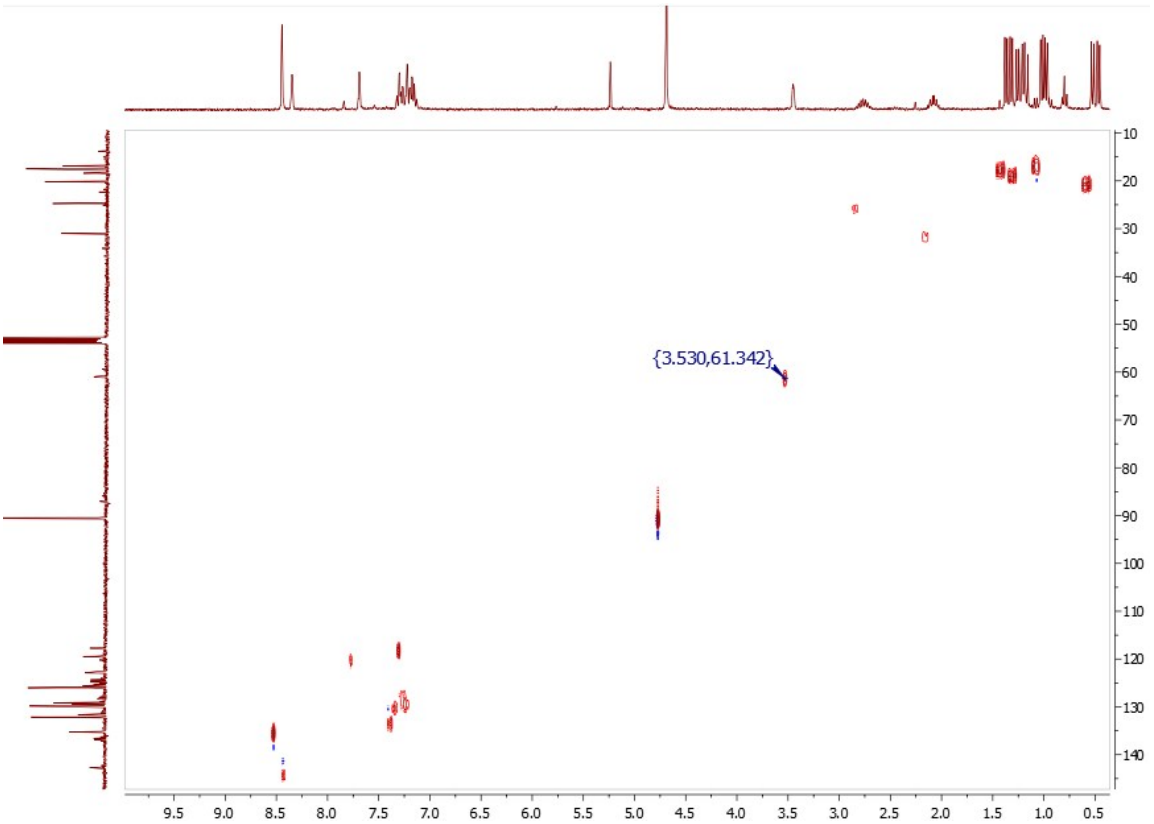

Figure S11. HSQC$\{^{1}H,^{13}C\}$ spectrum of **2** in CD_2Cl_2

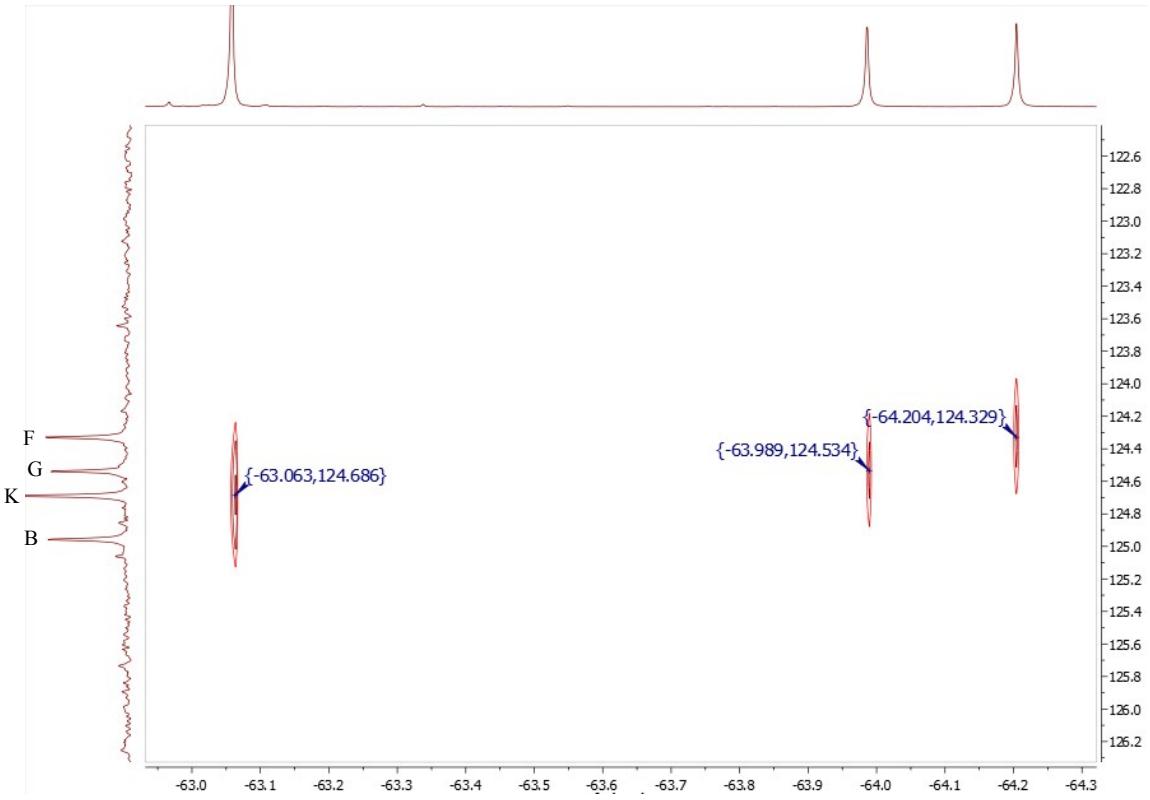

Figure S12. HSQC $\{^{13}C;^{19}F\}$ (J_{XH} = 280 Hz) spectrum of **2** in CD_2Cl_2. Projection along x-axis: $^{19}F\{^1H\}$, projection along y-axis: $^{13}C\{^1H,^{19}F\}$. Zoom CF_3 region.

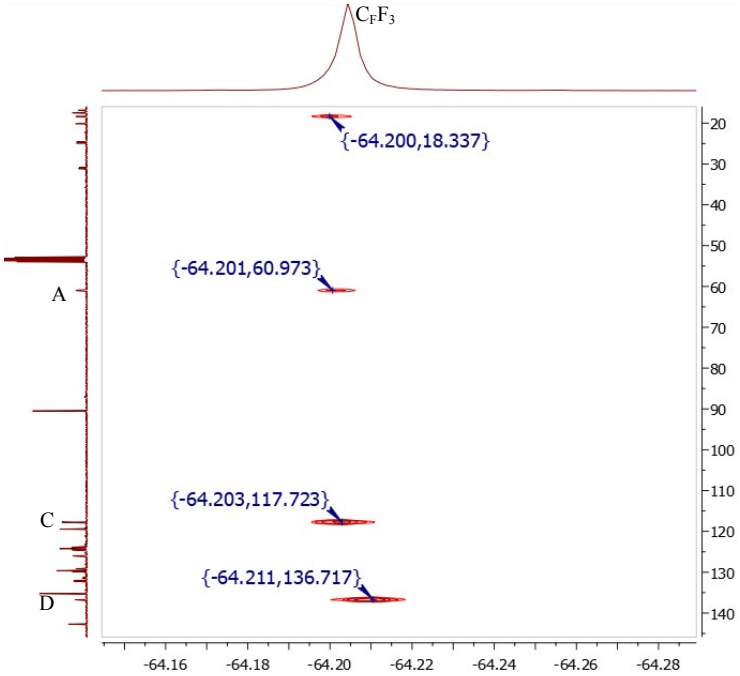

Figure S13. HSQC $\{^{13}C;^{19}F\}$ (J_{XH} = 10 Hz) spectrum of **2** in CD_2Cl_2. Projection along x-axis: $^{19}F\{^1H\}$, projection along y-axis: $^{13}C\{^1H,^{19}F\}$. Zoom C_FF_3 region.

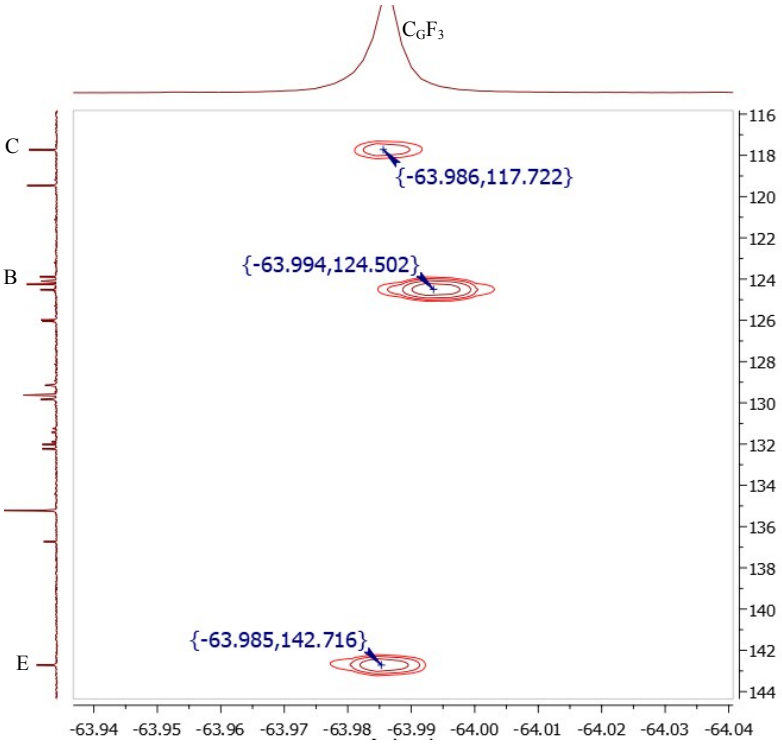

Figure S14. HSQC $\{^{13}C;^{19}F\}$ (J_{XH} = 10 Hz) spectrum of **2** in CD_2Cl_2. Projection along x-axis: $^{19}F\{^1H\}$, projection along y-axis: $^{13}C\{^1H,^{19}F\}$. Zoom C_GF_3 region.

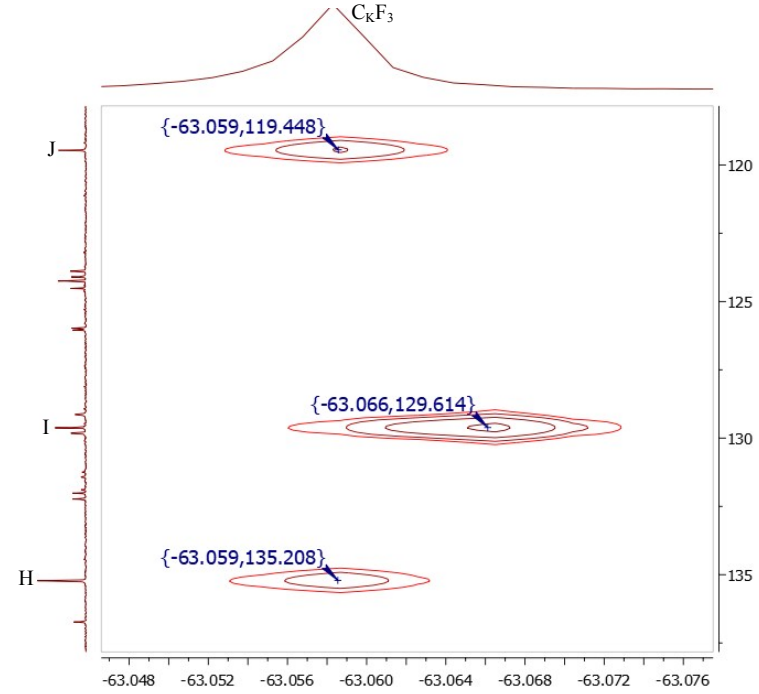

Figure S15. HSQC $\{^{13}C;^{19}F\}$ (J_{XH} = 10 Hz) spectrum of **2** in CD_2Cl_2. Projection along x-axis: $^{19}F\{^1H\}$, projection along y-axis: $^{13}C\{^1H,^{19}F\}$. Zoom C_KF_3 region.

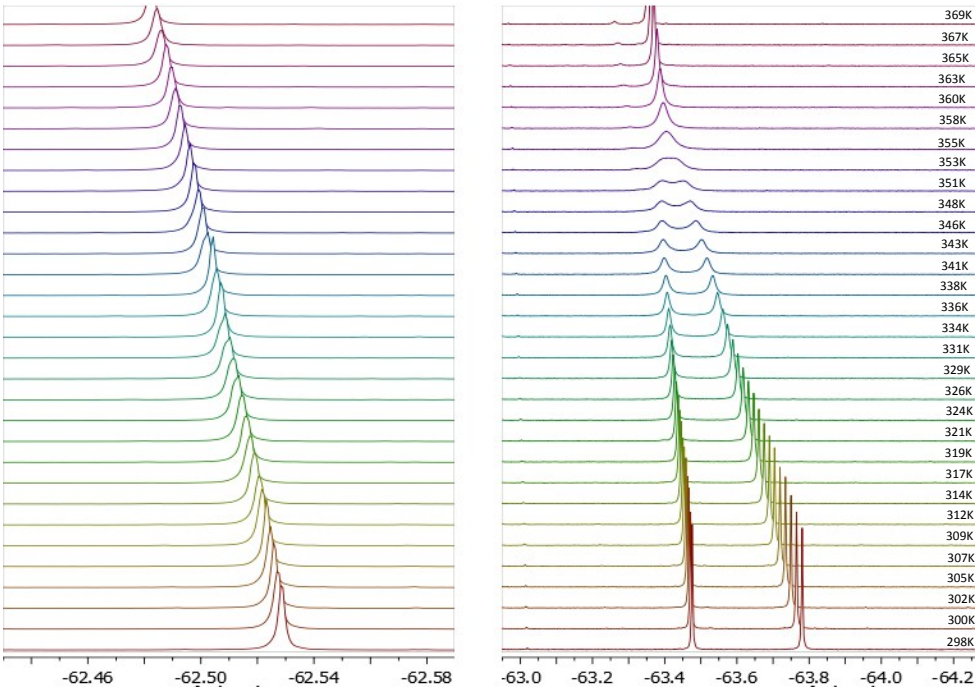

Figure S16. VT NMR $^{19}F\{^{1}H\}$ study of two CF_3 area in toluene-d_8.

Ethylene glycol was used as an external standard for the calibration of the temperature.[2]
The free energy of activation was estimated using the following formula:

$$\Delta G^{\neq} = RT_c \ln[RT_c\sqrt{2} / (\pi N_A h|\nu_A - \nu_B|)]$$

with R (gas constant), T_c (coalescence temperature), N_A (Avogadro's number), h (Planck's constant) and $|\nu_A-\nu_B|$ (chemical shift difference).
where T_c = 351 K and $|\nu_A-\nu_B|$ = 21 Hz; therefore $\Delta G^{\neq}$ **= 18.0 kcal.mol^{-1}**

[2] Ammann, C.; Meier, P.; Merbarch, A. *J. Magn. Reson.* **1982**, *46*, 319-321.

Synthesis of the (Cp)Rh(P,B)(PMe_3) complex **3**

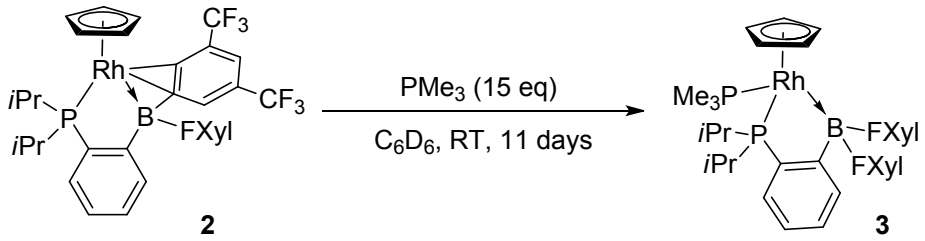

2 **3**

2 (20 mg, 0.025 mmol) was dissolved in 0.5 mL of C_6D_6 and charged in a pressure J. Young NMR tube. PMe_3 was added neat (38.6 µL, 0.375 mmol). The NMR tube was then left for 11 days. The excess of phosphine was removed under vacuum. Then the residue was re-dissolved in 0.5 mL of C_6D_6 and directly analysed by multinuclear NMR. X-Ray quality crystals were obtained by slow evaporation of a concentrated pentane solution.

NB: Higher temperatures gave less clean reactions. The excess of phosphine permitted to accelerate the reaction. Attempts to purify the complex led to degradation.

HRMS (ES-MS$^+$): exact mass (monoisotopic) calcd. for $[M]^+$ $(C_{36}H_{38}P_2F_{12}BRh)^+$: 874.1412; found, 874.1409.

^{1}H NMR (400 MHz, C_6D_6, 293K, δ): 0.19 (dd, 9H, $^2J_{HP}$ = 9.2 Hz, $^3J_{RhH}$ = 0.8 Hz, PMe_3), 0.92 (dd, $^3J_{HP}$ = 11.2 Hz, $^3J_{HH}$ = 7.2 Hz, 3H, CH_{3}*i*Pr), 0.93 (dd, $^3J_{HP}$ = 10.0 Hz, $^3J_{HH}$ = 7.6 Hz, 3H, CH_{3}*i*Pr), 0.95 (dd, $^3J_{HP}$ = 12.2 Hz, $^3J_{HH}$ = 8.0 Hz, 3H, CH_{3}*i*Pr), 1.15 (dd, 3H, $^3J_{HP}$ = 12.8 Hz, $^3J_{HH}$ = 6.8 Hz, CH_{3}*i*Pr), 1.70 (pseudo-oct, 1H, $^2J_{HP}$ = $^3J_{HH}$ = 7.2 Hz, CH*i*Pr), 2.31 (pseudo-oct, 1H, $^2J_{HP}$ = $^3J_{HH}$ = 7.2 Hz, CH*i*Pr), 4.80 (s, 5H, Cp), 6.96 (m, 1H, H_{arom}), 7.09 (m, 1H, H_{arom}), 7.27 (t, 1H, J_{HH} = 6.8 Hz, H_{arom}), 7.39 (d, 1H, J_{HH} = 7.6 Hz, H_{arom}), 7.62 (s br, 1H, $H_{Fxyl\ para}$), 7.68 (s br, 1H, $H_{Fxyl\ para}$), 8.09 (s br, 2H, $H_{Fxyl\ ortho}$), 8.43 (s br, 2H, $H_{Fxyl\ ortho}$)

^{13}C{^{1}H} NMR (100 MHz, C_6D_6, 293K, δ): 19.99 (s, CH_{3}*i*Pr), 21.05 (d, $^1J_{CP}$ = 30.3 Hz, PMe_3), 21.13 (s, CH_{3}*i*Pr), 21.42 (s, CH_{3}*i*Pr), 23.57 (s, CH_{3}*i*Pr), 26.59 (d, $^1J_{CP}$ = 21.6 Hz, CH*i*Pr), 35.60 (d, $^1J_{CP}$ = 22.2 Hz, CH*i*Pr), 92.53 (m, Cp), 117.33 (m, CH_{para} Fxyl), 117.88 (m, CH_{para} Fxyl), 124.79 (d, J_{CP} = 6.2 Hz, CH_{arom}), 125.16 (q, $^1J_{CF}$ = 271.3 Hz, $4CF_3$), 129.91 (s, CH_{arom}), 131.26 (s, CH_{arom}), 134.30 (s br, $2CH_{ortho}$ Fxyl), 135.23 (d, J_{CP} = 22.1 Hz, CH_{arom}), 135.46 (s br, $2CH_{ortho}$ Fxyl), 142.06 (d, $^1J_{CP}$ = 45.2 Hz, $C_{ipso}P$).

N.B.: $C_{ipso}B$ quaternary carbon atoms were not observed and *C*-CF_3 carbons are under the residual signal of benzene.

N.B.: Impurity signals in the aliphatic area are due to the use of an excess of PMe_3.

^{11}B NMR (128.4 MHz, C_6D_6, 293K, δ): 4.58 (s br)

^{31}P{^{1}H} NMR (121 MHz, C_6D_6, 293K, δ): -2.45 (dd, $^2J_{PP}$ = 50.3 Hz, $^1J_{PRh}$ = 179.9 Hz, PMe_3), 81.22 (dd, $^2J_{PP}$ = 50.0 Hz, $^1J_{PRh}$ = 169.3 Hz, P*i*Pr$_2$)

^{19}F{^{1}H} NMR (282.4 MHz, C_6D_6, 293K, δ): -62.46 (s, $2CF_3$), -62.33 (s, $2CF_3$).

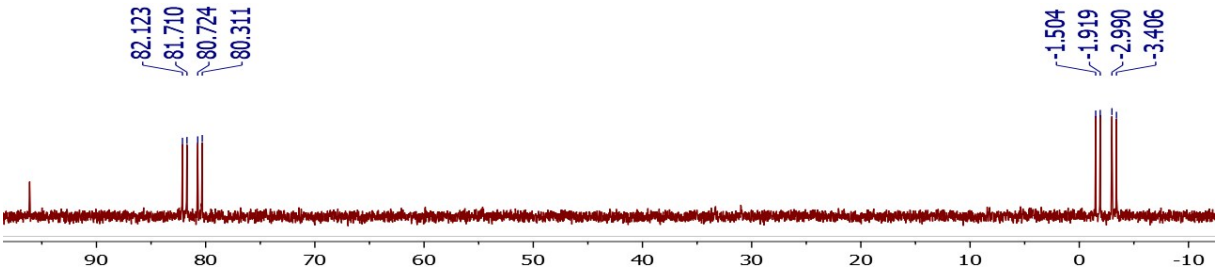

Figure S17. ^{31}P NMR spectrum of **3** (121 MHz, 293K) in C_6D_6

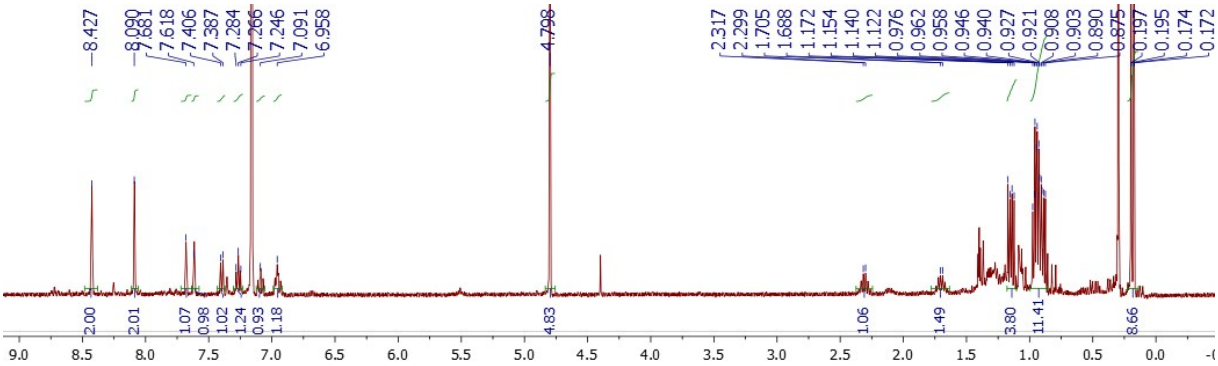

Figure S18. ^{1}H NMR spectrum of **3** (400 MHz, 293K) in C_6D_6

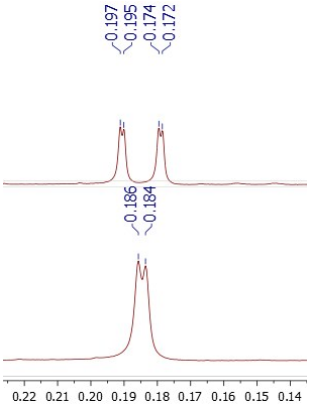

Figure S19. ^{1}H NMR spectrum of **3** (400 MHz, 293K) in C_6D_6, PMe_3 region. Top ^{1}H, bottom $^{1}H\{^{31}P\}$ O2p = 0 ppm.

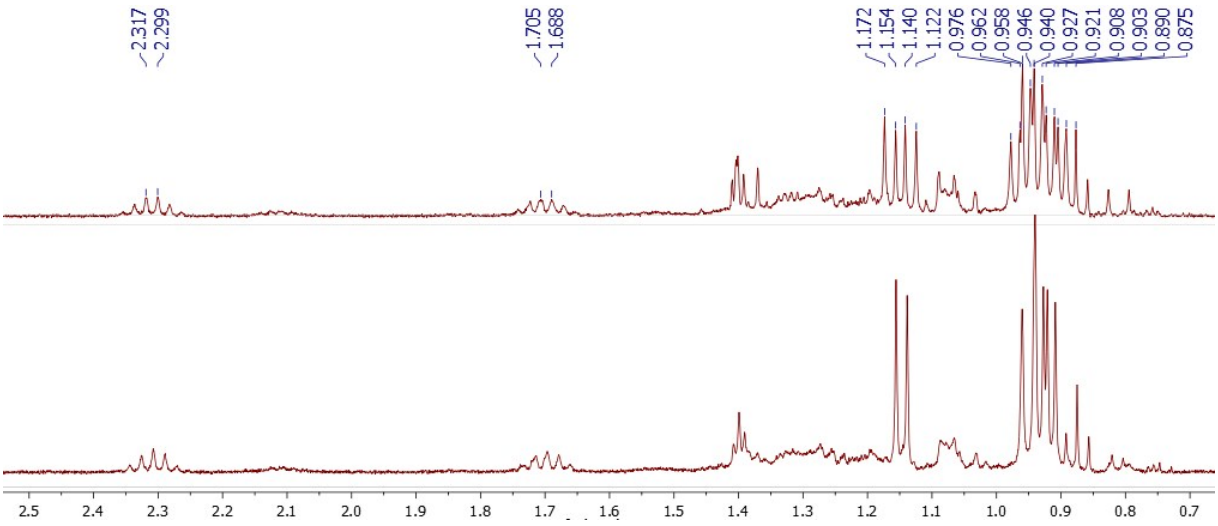

Figure S20. ^{1}H NMR spectrum of **3** (400 MHz, 293K) in C_6D_6, aliphatic region. Top ^{1}H, bottom $^{1}H\{^{31}P\}$ O2p = 80 ppm.

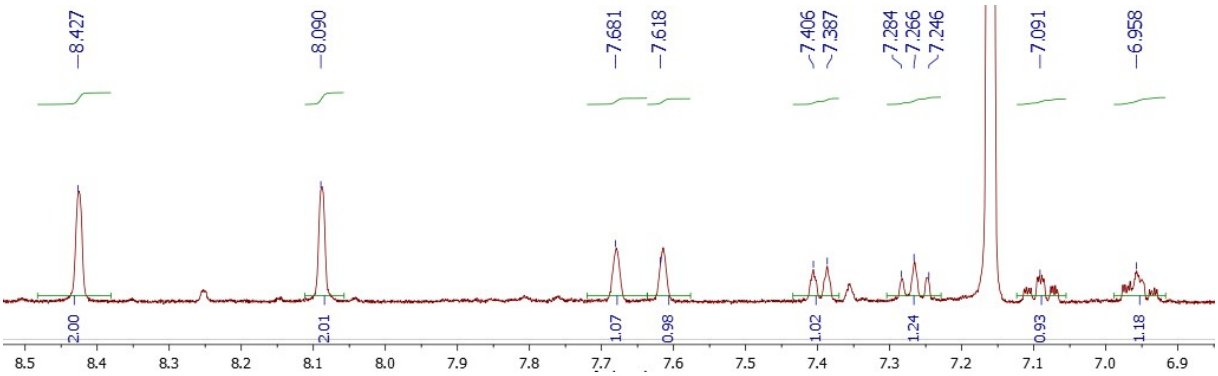

Figure S21. ^{1}H NMR spectrum of **3** (400 MHz, 293K) in C_6D_6, aromatic region

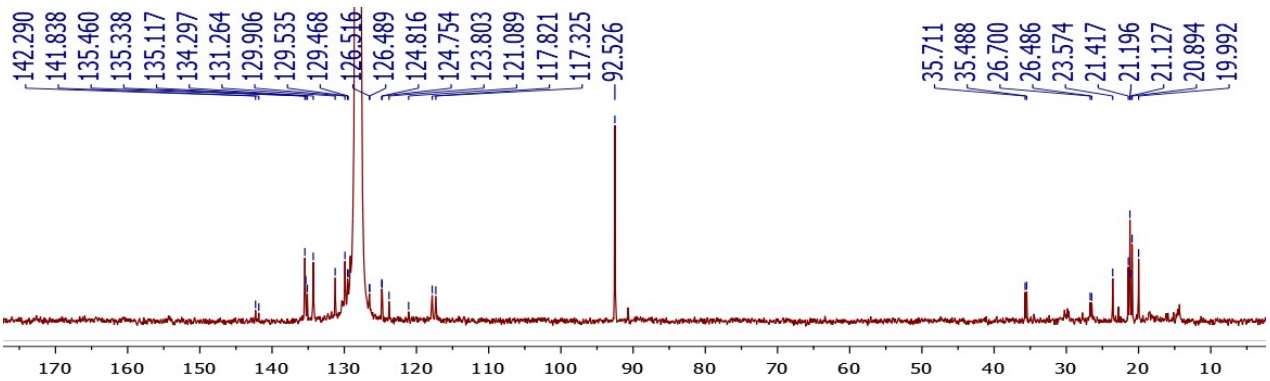

Figure S22. ^{13}C NMR spectrum of **3** (100 MHz, 293K) in C_6D_6

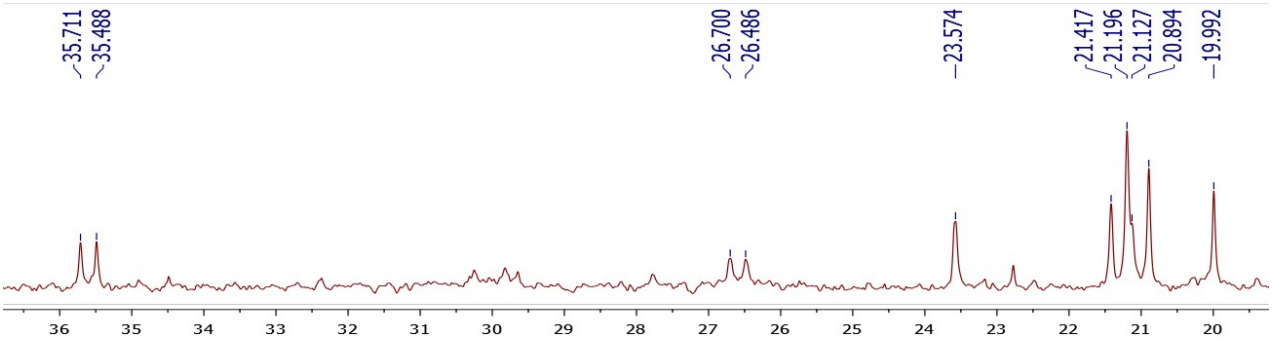

Figure S23. ^{13}C NMR spectrum of **3** (100 MHz, 293K) in C_6D_6, aliphatic region

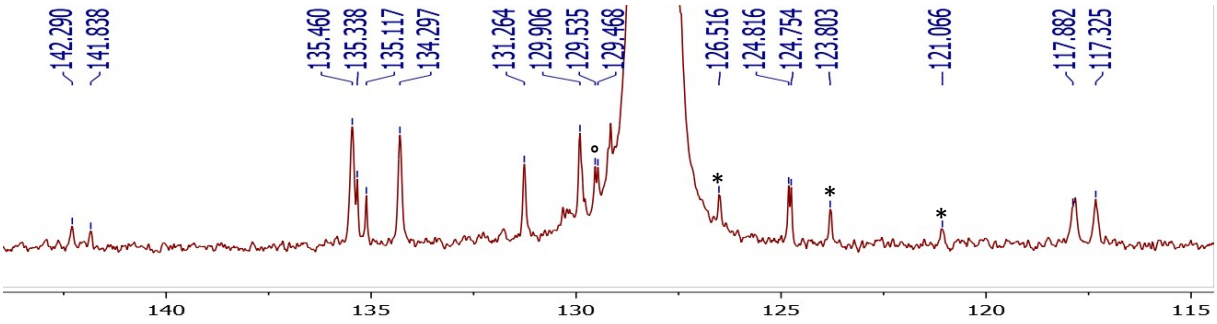

° *C*-CF_3 carbons, * *C*F_3 carbons.

Figure S24. ^{13}C NMR spectrum of **3** (100 MHz, 293K) in C_6D_6, aromatic region

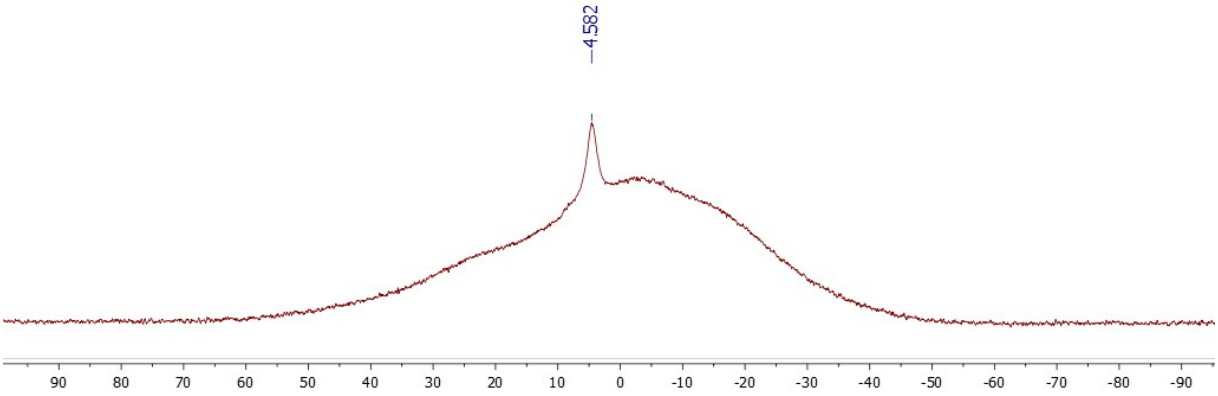

Figure S25. ^{11}B NMR spectrum of **3** (128.4 MHz, 293K) in C_6D_6

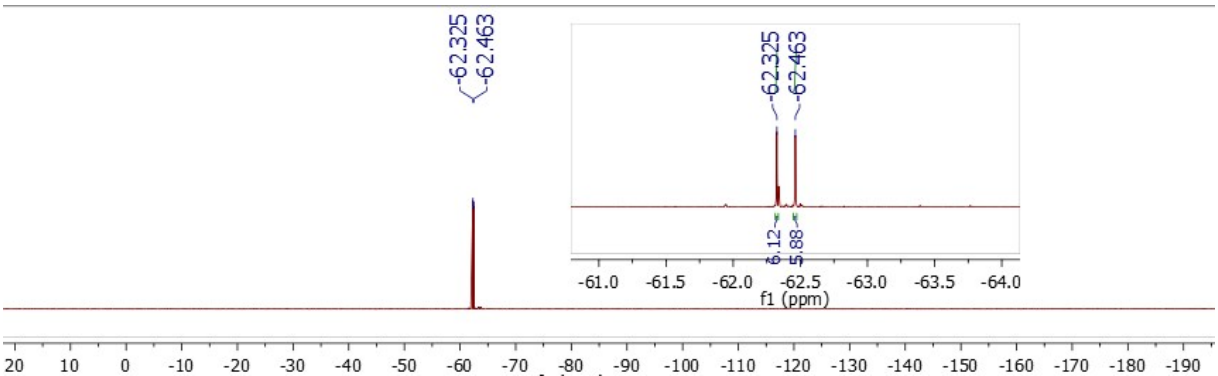

Figure S26. ^{19}F NMR spectrum of **3** (282.4 MHz, 293K) in C_6D_6

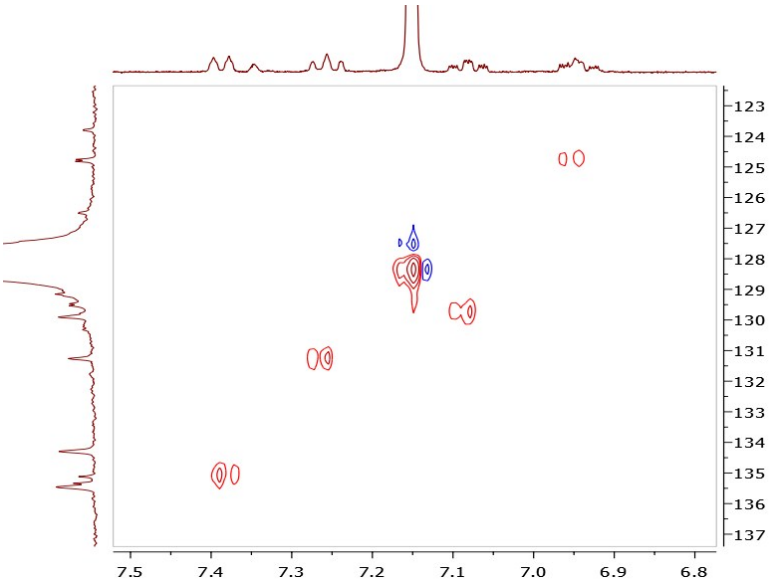

Figure S27. HSQC of **3** in C_6D_6, CH_{arom} region

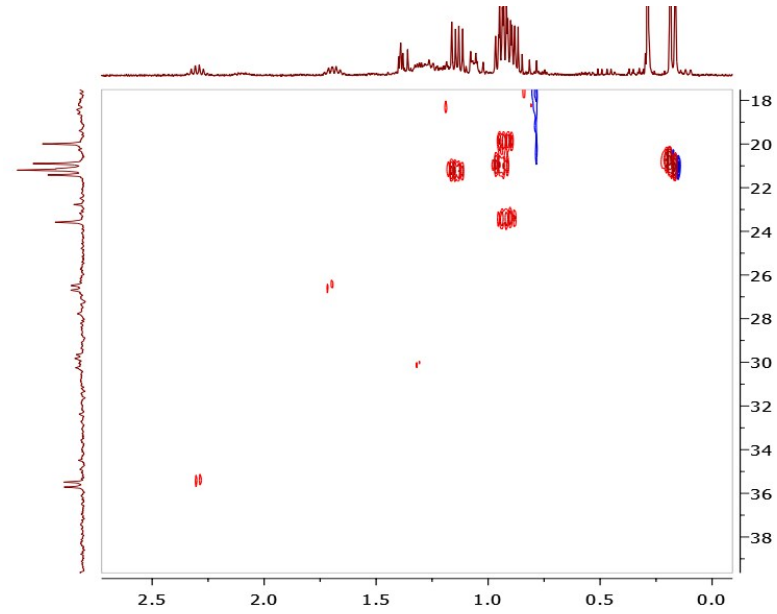

Figure S28. HSQC of **3** in C_6D_6, aliphatic region

Synthesis of the (Cp)Rh(P,B)(CNXyl) complex **4**

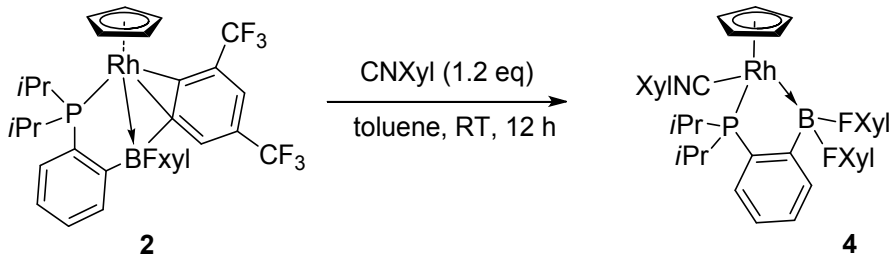

2 **4**

2 (20 mg, 0.025 mmol) and CNXyl (4 mg, 0.030 mmol) were dissolved in 0.5 mL of toluene and charged in a J. Young NMR tube. After 12 hours, the clear yellow solution was evaporated to afford a fluffy yellow solid. The solid was washed with 0.2 mL of pentane in order to remove the excess of CNXyl. After drying under vacuum, 19.7 mg of a yellow powder were obtained (85% yield). X-Ray quality crystals were obtained by slow evaporation of a concentrated pentane solution at room temperature.

HRMS (ES-MS$^+$): exact mass (monoisotopic) calcd. for $[M]^+$ $(C_{42}H_{38}PF_{12}BNRh)^+$: 929.1705; found, 929.1691.

m.p.: 166 °C (decomp.).

IR (DCM): ν_{NC} = 2019 cm^{-1}

^{1}H NMR (400 MHz, C_6D_6, 293K, δ): 0.79 (dd, 3H, $^3J_{HP}$ = 15.6 Hz, $^3J_{HH}$ = 7.2 Hz, CH_{3iPr}), 0.82 (dd, 3H, $^3J_{HP}$ = 13.2 Hz, $^3J_{HH}$ = 7.2 Hz, CH_{3iPr}), 0.87 (dd, 3H, $^3J_{HP}$ = 13.2 Hz, $^3J_{HH}$ = 6.8 Hz, CH_{3iPr}), 0.91 (pseudo t, 3H, $^3J_{HP}$ = 13.2 Hz, $^3J_{HH}$ = 6.4 Hz, CH_{3iPr}), 1.56 (s, 6H, CH_3 Xyl), 1.97 (m, 1H, CH_{iPr}), 2.19 (m, 1H, CH_{iPr}), 5.11 (s, 5H, Cp), 6.56 (d, 2H, J_{HH} = 7.6 Hz, H_{arom}), 6.68 (m, 1H, H_{arom}), 6.92 (m, 1H, H_{arom}), 7.05 (m, 2H, H_{arom}), 7.43 (m, 1H, H_{arom}), 7.52 (s br, 1H, $H_{Fxyl\ para}$), 7.62 (s br, 1H, $H_{Fxyl\ para}$), 8.05 (s br, 2H, $H_{Fxyl\ ortho}$), 8.27 (s br, 2H, $H_{Fxyl\ ortho}$).

^{13}C{^{1}H} NMR (100 MHz, C_6D_6, 293K, δ): 18.08 (s, 2 CH_3 Xyl), 18.19 (d, $^2J_{CP}$ = 3.8 Hz, CH_{3iPr}), 20.19 (d, $^2J_{CP}$ = 2.3 Hz, CH_{3iPr}), 20.33 (d, $^2J_{CP}$ = 2.8 Hz, CH_{3iPr}), 20.92 (s, CH_{3iPr}), 24.51 (d, $^1J_{CP}$ = 28.0 Hz, CH_{iPr}), 30.81 (d, $^1J_{CP}$ = 21.0 Hz, CH_{iPr}), 92.29 (m, Cp), 117.95 (m, CH_{para} Fxyl), 118.19 (m, CH_{para} Fxyl), 124.75 (d, J_{CP} = 7.0 Hz, CH_{arom}), 124.89 (q, $^1J_{CF}$ = 271.0 Hz, CF_3), 125.02 (q, $^1J_{CF}$ = 271.0 Hz, CF_3), 129.39 (q, $^2J_{CF}$ = 31.5 Hz, *C*-CF_3), 129.50 (q, $^2J_{CF}$ = 31.5 Hz, *C*-CF_3), 130.14 (m, 2CH_{arom}), 133.78 (d, J_{CP} = 21.0 Hz, CH_{arom}), 133.81 (s, C_{quat} Xyl), 134. 37 (m, 2 CH_{ortho} Fxyl), 134.98 (m, 2CH_{ortho} Fxyl), 140.91 (dd, $^1J_{CP}$ = 51.5 Hz, $^2J_{CRh}$ = 3.0 Hz, C_{ipso}-P), 158.62 (dd, $^1J_{CRh}$ = 84.0 Hz, $^2J_{CP}$ = 24.4 Hz, *C*NXyl), 161.41 (br, C_{ipso}B), 162.29 (br, C_{ipso}B), 167.05 (br, C_{ipso}B).

N.B.: Two aromatic CH carbon atoms are under the residual signal of C_6D_6.

^{11}B NMR (128.4 MHz, C_6D_6, 293K, δ): 8.75.

^{31}P{^{1}H} NMR (121 MHz, C_6D_6, 293K, δ): 84.46 (d, $^1J_{PRh}$ = 173.0 Hz).

^{19}F NMR (282.4 MHz, C_6D_6, 293K, δ): -62.56 (s, 2CF_3), -62.29 (s, 2CF_3).

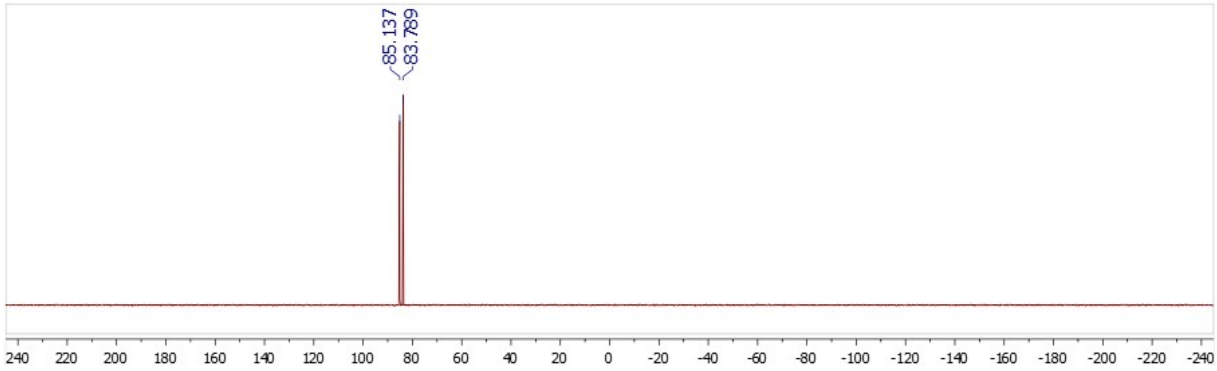

Figure S29. $^{31}P\{^{1}H\}$ NMR spectrum of **4** (128 MHz, 293K) in C_6D_6

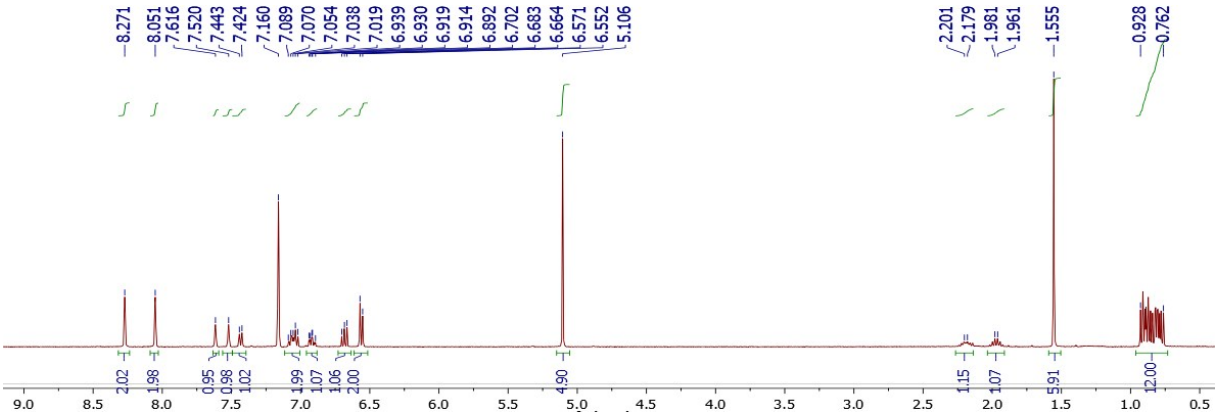

Figure S30. ^{1}H NMR spectrum of **4** (400 MHz, 293K) in C_6D_6

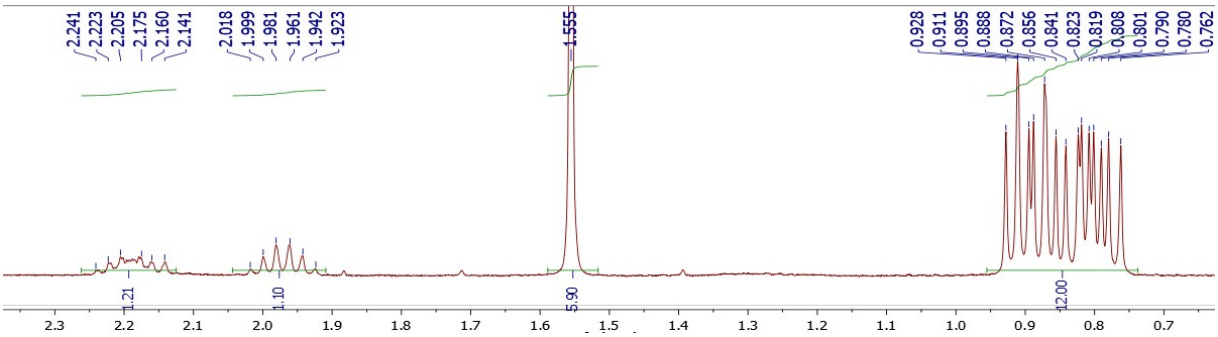

Figure S31. ^{1}H NMR spectrum of **4** (300 MHz, 293K) in C_6D_6; aliphatic region

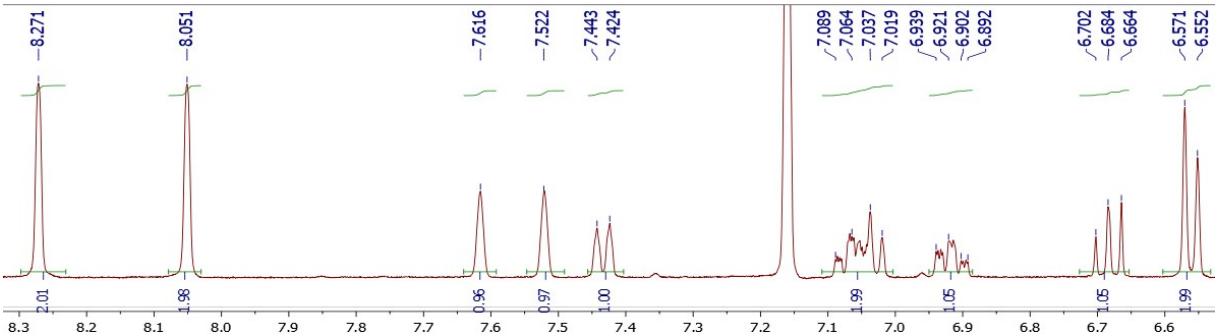

Figure S32. ^{1}H NMR spectrum of **4** (300 MHz, 293K) in C_6D_6; aromatic region

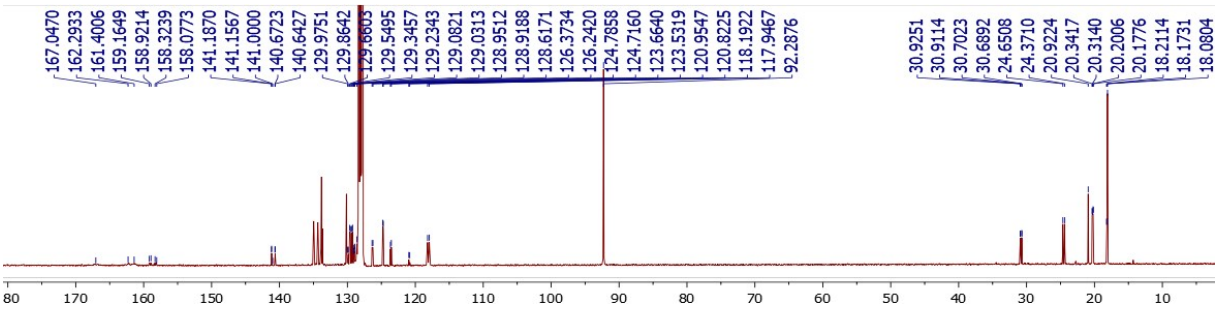

Figure S33. $^{13}C\{^{1}H\}$ spectrum of **4** (100 MHz, 293K) in C_6D_6

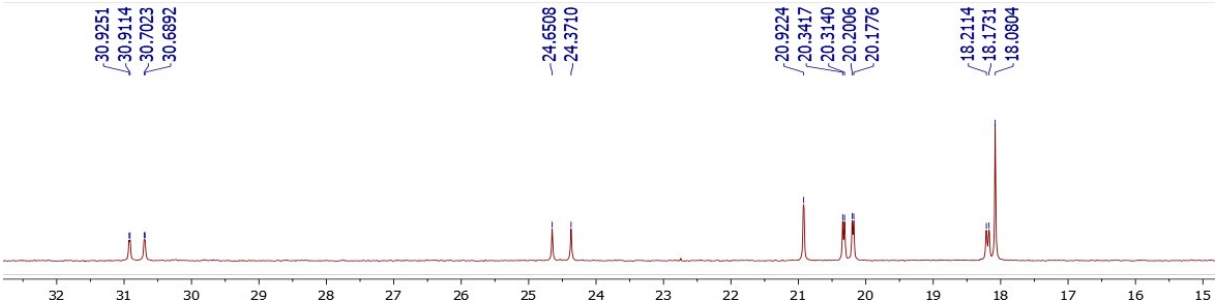

Figure S34. $^{13}C\{^{1}H\}$ spectrum of **4** (100 MHz, 293K) in C_6D_6; aliphatic region

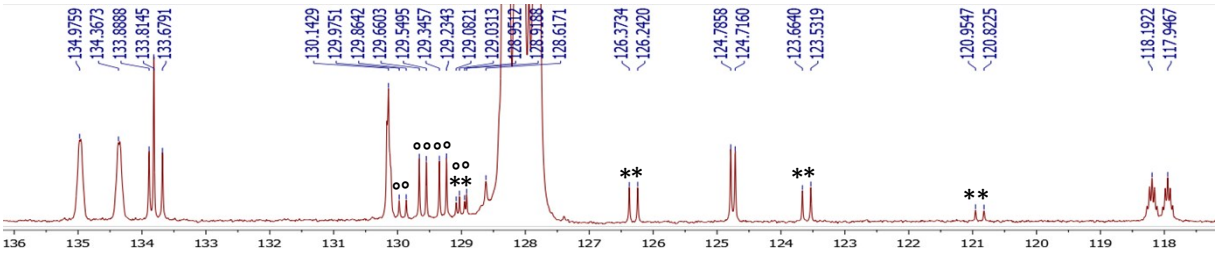

° *C*-CF_3 carbons, * *C*F_3 carbons.

Figure S35. $^{13}C\{^{1}H\}$ spectrum of **4** (100 MHz, 293K) in C_6D_6; aromatic region

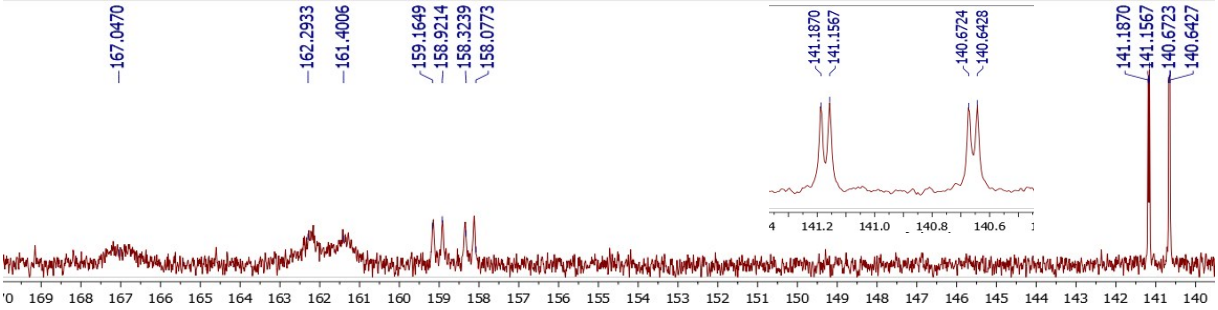

Figure S36. $^{13}C\{^{1}H\}$ spectrum of **4** (100 MHz, 293K) in in C_6D_6; quaternary carbons region

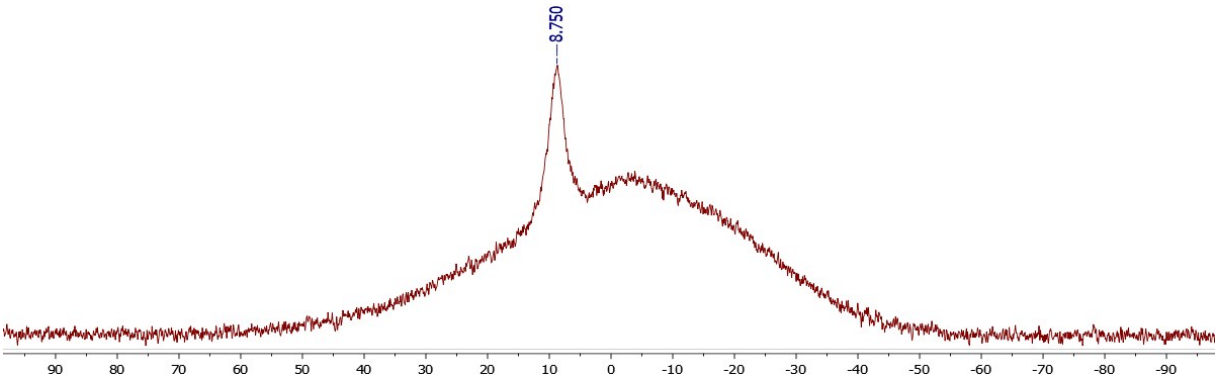

Figure S37. ^{11}B NMR spectrum of **4** (128.4 MHz, 293K) in C_6D_6

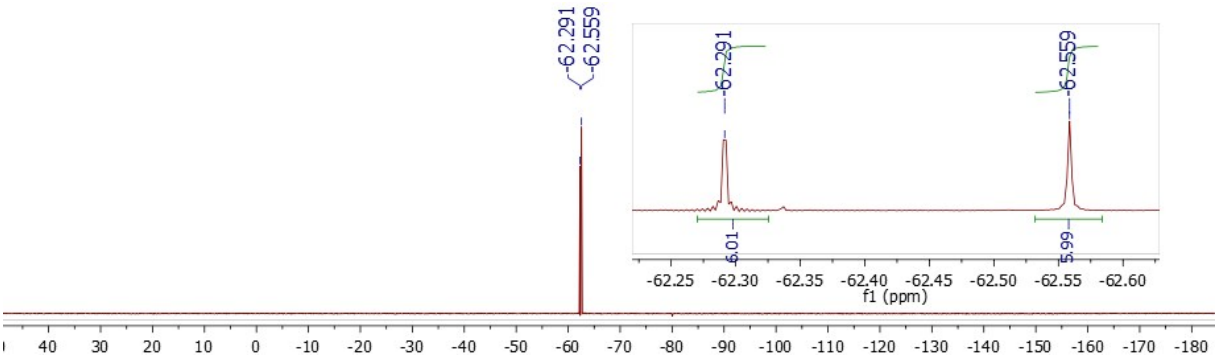

Figure S38. ^{19}F spectrum of **4** (282.4 MHz, 293K) in C_6D_6

Synthesis of the (Cp)Rh(P,B)(CO) complex **5**

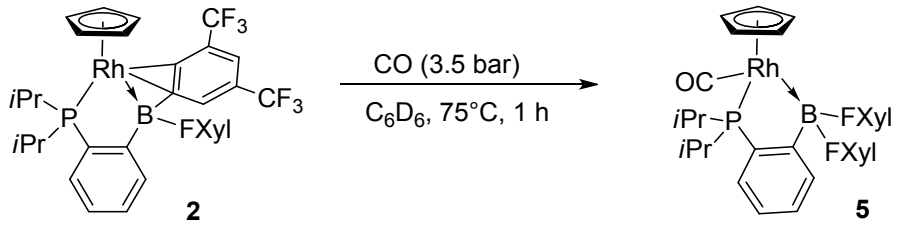

2 (20 mg, 0.025 mmol) was dissolved in 0.5 mL of C_6D_6 and charged in a pressure J. Young NMR tube. The reaction mixture was degassed via freeze pump thaw three times, then submitted to 3.5 bar of CO. The NMR tube was then heated to 75°C for one hour, and the solution became clear yellow. It was then degassed by freeze-pump-thaw and directly analysed by multinuclear NMR.

NB: The complex is stable enough to remove the excess of CO under vacuum, but it gives back 30% of the starting complex after 12 hours under dynamic vacuum.

HRMS (CI-CH_4): exact mass (monoisotopic) calcd. for $[M+H]^+$ $(C_{34}H_{30}BF_{12}OPRh)^+$: 827.0991; found, 827.1010.

IR (DCM): ν_{CO} = 2011 cm^{-1}

^1H NMR (500 MHz, C_6D_6, 293K, δ): 0.64 (dd, 3H, $^3J_{HP}$ = 16.5 Hz, $^3J_{HH}$ = 7.5 Hz, CH_{3iPr}), 0.69 (dd, 3H, $^3J_{HP}$ = 17.0 Hz, $^3J_{HH}$ = 7.0 Hz, CH_{3iPr}), 0.70 (dd, 3H, $^3J_{HP}$ = 15.0 Hz, $^3J_{HH}$ = 7.0 Hz, CH_{3iPr}), 0.78 (dd, 3H, $^3J_{HP}$ = 16.0 Hz, $^3J_{HH}$ = 7.0 Hz, CH_{3iPr}), 1.90 (m, 2H, CH_{iPr}), 4.71 (s, 5H, Cp), 6.90 (m, 2H, H_{arom}), 7.02 (m, 1H, H_{arom}), 7.14 (m, 1H, H_{arom}), 7.61 (s br, 1H, $H_{Fxyl\ para}$), 7.75 (s br, 1H, $H_{Fxyl\ para}$), 8.05 (s br, 2H, $H_{Fxyl\ ortho}$), 8.18 (s br, 2H, $H_{Fxyl\ ortho}$).

$^{13}C\{^1H\}$ NMR (125.8 MHz, C_6D_6, 293K, δ): 18.60 (s, CH_{3iPr}), 19.41 (s, CH_{3iPr}), 19.61 (s, CH_{3iPr}), 19.93 (d, $^2J_{CP}$ = 3.0 Hz CH_{3iPr}), 26.51 (d, $^1J_{CP}$ = 30.0 Hz, CH_{iPr}), 32.56 (d, $^1J_{CP}$ = 23.0 Hz, CH_{iPr}), 93.34 (m, Cp), 118.81 (m, CH_{para} Fxyl), 118.96 (m, CH_{para} Fxyl), 124.79 (q, $^1J_{CF}$ = 272.0 Hz, CF_3), 124.93 (q, $^1J_{CF}$ = 273.0 Hz, CF_3), 125.84 (d, J_{CP} = 5.9 Hz, CH_{arom}), 129.70 (m, CH_{arom}), 129.86 (q, $^2J_{CF}$ = 32.0 Hz, *C*-CF_3), 130.38 (q, $^2J_{CF}$ = 32.0 Hz, *C*-CF_3), 130.72 (d, J_{CP} = 2.4 Hz, CH_{arom}), 134.20 (d, J_{CP} = 22.0 Hz, CH_{arom}), 134.77 (m, CH_{ortho} Fxyl), 135.09 (m, CH_{ortho} Fxyl), 138.66 (dd, $^1J_{CP}$ = 51.3 Hz, $^2J_{CRh}$ = 2.6 Hz, $C_{ipso}P$), 192.36 (dd, $^1J_{CRh}$ = 81.6 Hz, $^2J_{CP}$ = 21.0 Hz, CO). N.B.: $C_{ipso}B$ quaternary carbon atoms were not observed.

^{11}B NMR (128.4 MHz, CD_2Cl_2, 293K, δ): 14.01 (s br).

$^{31}P\{^1H\}$ NMR (121 MHz, CD_2Cl_2, 293K, δ): 84.26 (d, $^1J_{PRh}$ = 169.0 Hz).

^{19}F NMR (282.4 MHz, CD_2Cl_2, 293K, δ): -62.59 (s, CF_3), -62.41 (s, CF_3).

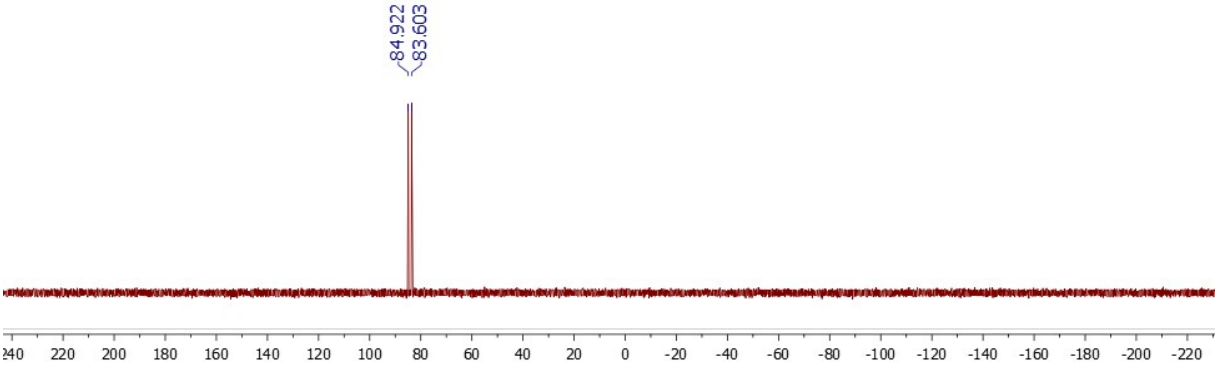

Figure S39. $^{31}P\{^{1}H\}$ NMR spectrum of **5** (128 MHz, 293K) in C_6D_6

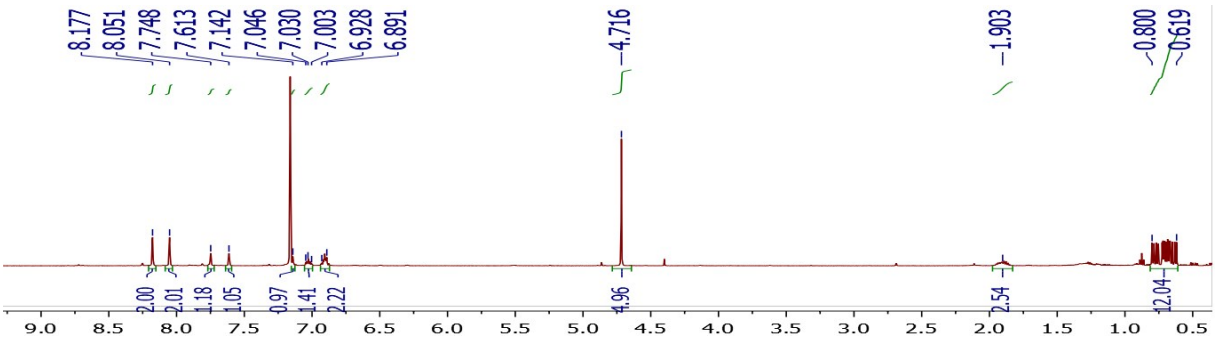

Figure S40. ^{1}H NMR spectrum of **5** (500 MHz, 293K) in C_6D_6

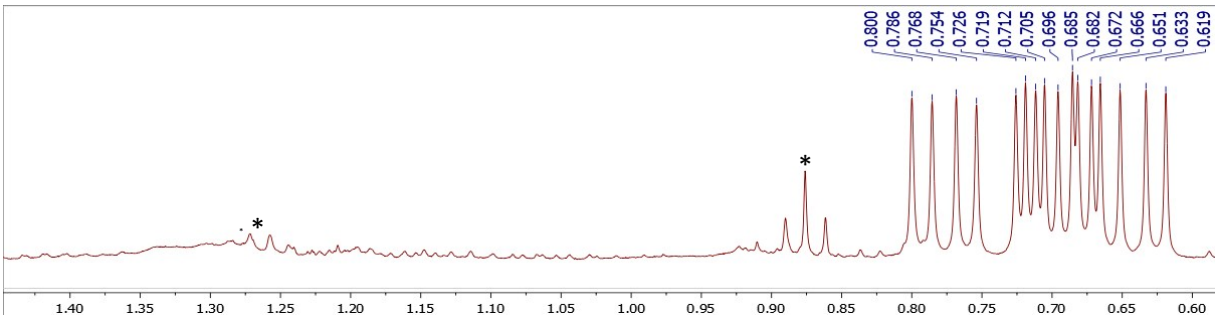

* Pentane

Figure S41. ^{1}H NMR spectrum of **5** (500 MHz, 293K) in C_6D_6; aliphatic region

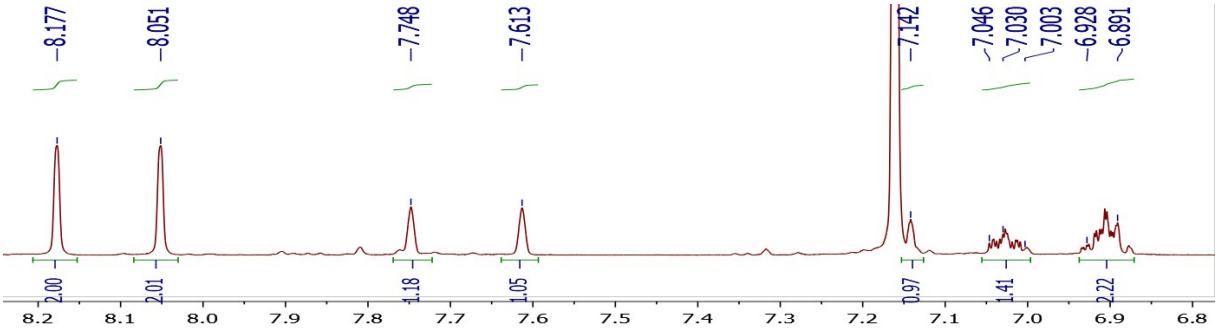

Figure S42. ^{1}H NMR spectrum of **5** (500 MHz, 293K) in C_6D_6; aromatic region

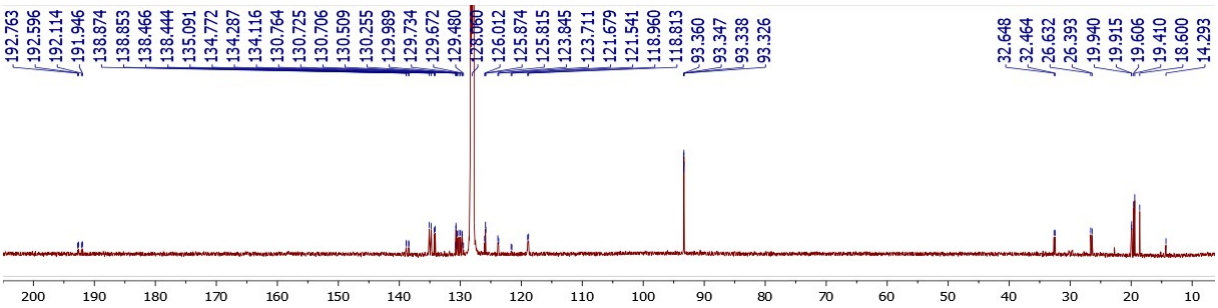

Figure S43. $^{13}C\{^{1}H\}$ spectrum of **5** (125.8 MHz, 293K) in C_6D_6

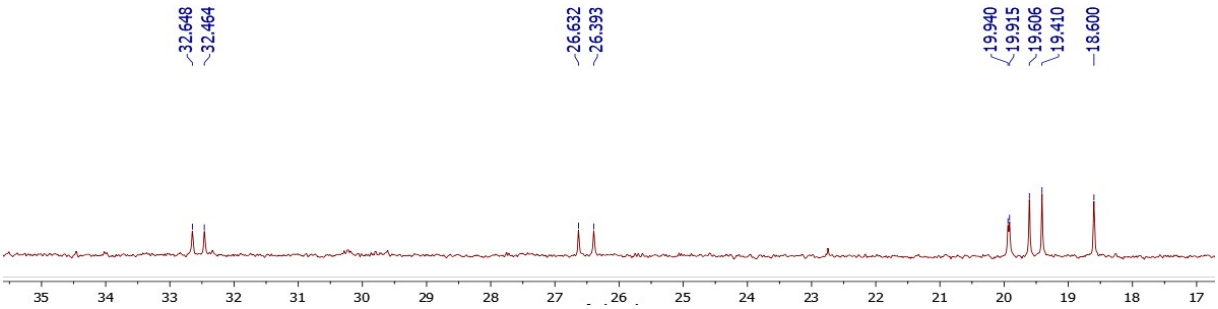

Figure S44. $^{13}C\{^{1}H\}$ spectrum of **5** (125.8 MHz, 293K) in C_6D_6; aliphatic region

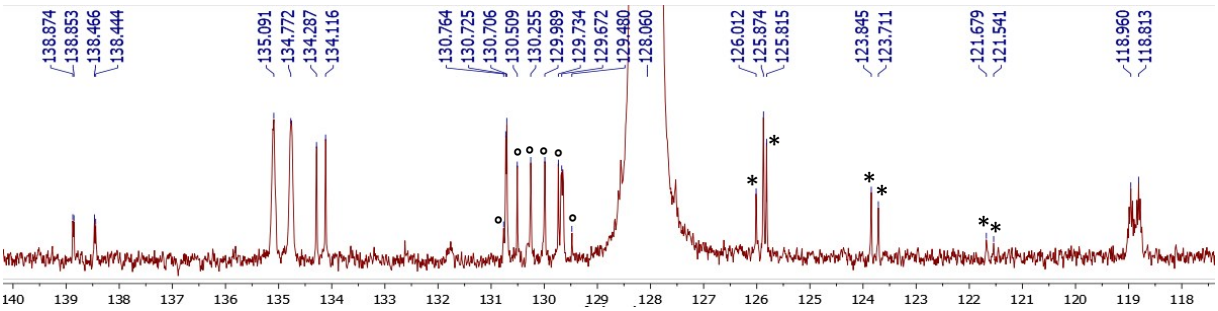

° *C*-CF_3 carbon atoms, * *C*F_3 carbon atoms.

Figure S45. $^{13}C\{^{1}H\}$ spectrum of **5** (125.8 MHz, 293K) in C_6D_6; aromatic region

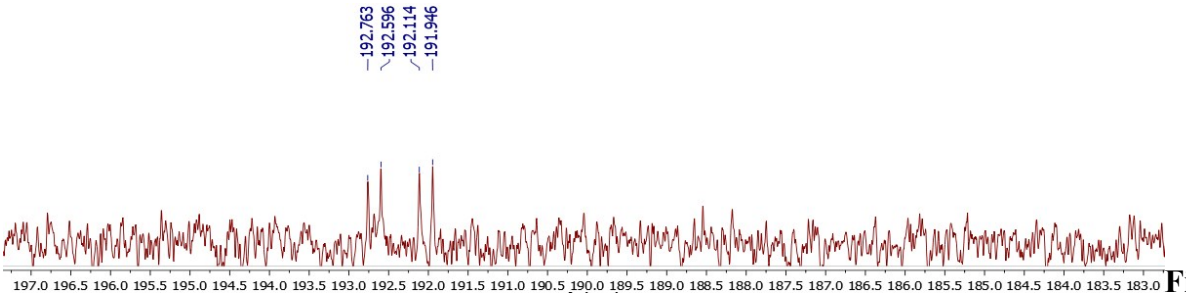

Figure S46. ^{13}C spectrum of **5** (125.8 MHz, 293K) in C_6D_6; CO region

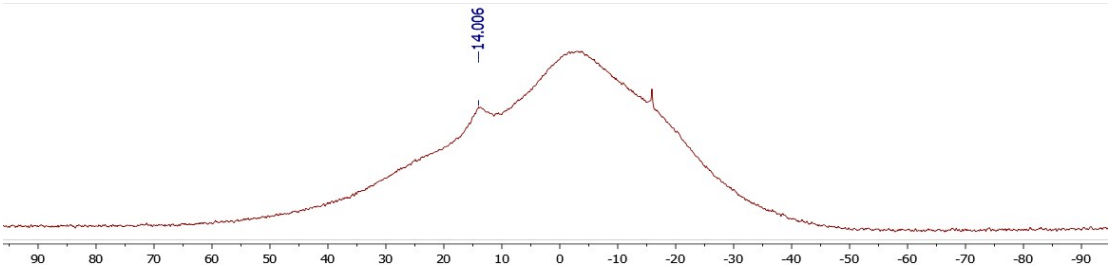

Figure S47. ^{11}B NMR spectrum of **5** (128.4 MHz, 293K) in C_6D_6

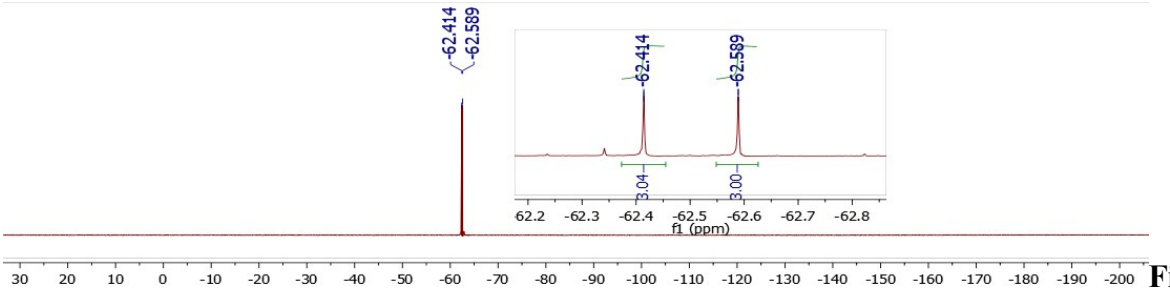

Figure S48. ^{19}F spectrum of **5** (282.4 MHz, 293K) in C_6D_6

Crystallographic data

Crystallographic data were collected at low temperature (193(2)) on a Bruker-AXS APEXII QUAZAR diffractometer equipped with a 30W air-cooled microfocus source (MoK_α radiation, λ = 0.71073 Å). Phi- and omega- scans were used. An empirical absorption correction was employed.[2] The structures were solved by intrinsic phasing method[3] and refined by the least-squares method on F^2.[4] All non-hydrogen atoms were refined with anisotropic displacement parameters and the hydrogen atoms were refined isotropically. The hydrogen atoms were refined at calculated positions using the riding model.

CCDC 1938717 (**2**), 1938718 (**3**) and 1938719 (**4**) contain the supplementary crystallographic data for this paper. These data can be obtained free of charge from The Cambridge Crystallographic Data Centre.

2: $C_{33}H_{29}BF_{12}PRh$, M = 798.25, monoclinic, $P2_1/n$, a = 13.0614(9) Å, b = 12.3133(6) Å, c = 20.7087(13) Å, $\alpha = \gamma = 90°$, β = 105.427(4)°, V = 3210.6(3) Å^3, Z = 4, crystal size 0.10 x 0.04 x 0.02 mm^3, 35921 reflections collected (8274 independent, R_{int} = 0.0844), 554 parameters, $R1$ [I>2σ(I)] = 0.0472, $wR2$ [all data] = 0.1196, largest diff. peak and hole: 0.752 and -0.655 eÅ^{-3}.

3: $C_{36}H_{38}BF_{12}P_2Rh$, M = 874.32, monoclinic, $P2_1/n$, a = 14.0294(5) Å, b = 17.6591(7) Å, c = 15.1340(6) Å, $\alpha = \gamma = 90°$, β = 105.427(4)°, V = 3738.8(2) Å^3, Z = 4, crystal size 0.10 x 0.08 x 0.06 mm^3, 36863 reflections collected (6553 independent, R_{int} = 0.0566), 551 parameters, $R1$ [I>2σ(I)] = 0.0387, $wR2$ [all data] = 0.0954, largest diff. peak and hole: 0.686 and -0.507 eÅ^{-3}.

4: $C_{42}H_{38}BF_{12}NPRh$, M = 929.42, monoclinic, $P2_1/c$, a = 11.1009(10) Å, b = 19.504(2) Å, c = 18.980(2) Å, $\alpha = \gamma = 90°$, β = 100.359(3)°, V = 4042.6(7) Å^3, Z = 4, crystal size 0.14 x 0.06 x 0.04 mm^3, 94983 reflections collected (9997 independent, R_{int} = 0.0654), 594 parameters, $R1$ [I>2σ(I)] = 0.0356, $wR2$ [all data] = 0.0891, largest diff. peak and hole: 0.642 and -0.506 eÅ^{-3}.

[2] Bruker, *SADABS*, Bruker AXS Inc., Madison, Wisconsin, USA.
[3] G. M. Sheldrick *Acta Cryst*. **2015**, A71, 3–8.
[4] G. M. Sheldrick *Acta Cryst. A* **2008**, *64*, 112–122.